ACCURACY OF SUSCEPTIBILITY WEIGHTED IMAGING AND 3D-TOF MRA IN DETECTION AND PRE-TREATMENT EVALUATION OF INTRACRANIAL DURAL ARTERIOVENOUS FISTULAS

Minth Punpichet, Poonperm Sucharitpong*, Norraseth Kittinorraseth*, Sujima Tangjintanakan*, Supakajee Saengruang-Orn***

*** Department of Radiology, Phramongkutklao Hospital, Bangkok, Thailand**
**** Department of Radiology, Division of Academic Affairs, Phramongkutklao College of Medicine, Bangkok, Thailand**

Abstract

Background: Dural arteriovenous fistulas (DAVFs) are abnormal connections between meningeal arteries and dural venous sinuses or cortical veins. A cerebral angiogram is the gold standard for diagnosing and treating DAVFs. Still, non-invasive techniques such as three-dimensional time-of-flight magnetic resonance angiography (3D-TOF MRA) and susceptibility-weighted imaging (SWI) are also helpful in evaluating the location and severity of the fistulas, including cortical venous reflux (CVR) and cortical venous ectasia (CVE). This study aimed to compare the efficacy in detecting and pretreating DAVFs evaluating SWI and 3D-TOF MRA with cerebral angiography.

Methods: The retrospective study included 35 patients with 41 DAVFs who underwent pre-treatment MR imaging and cerebral angiogram. The fistulous point at convexity and cavernous locations, arterial feeders, venous drainers, CVR, and CVE were evaluated.

Results: SWI and 3D-TOF MRA showed high sensitivity and excellent specificity in detecting DAVFs Cognard II-IV at convexity location and high sensitivity in evaluating CVR. For DAVFs at cavernous sinus locations, arterial feeders and venous drainers were significantly identified in 3D-TOF MRA ($p < 0.001$). SWI exhibited superior sensitivity (87.5%) in detecting CVE at convexity locations ($p < 0.001$). Slow flow or low-grade fistulas in cavernous sinus locations (n = 2, 4.8%, Cognard I) were not identified using MR imaging.

Conclusion: SWI and 3D-TOF MRA are helpful tools for evaluating high-flow DAVFs (Cognard II-IV). SWI is superior in detecting CVE in convexity locations but is limited in assessing the fistulous point in cavernous sinus locations. Thus, combining findings from both SWI and 3D-TOF MRA exhibited high accuracy in detecting and pretreating high-flow DAVFs.

Keywords: dural arteriovenous fistulas (DAVFs), three-dimensional time-of-flight magnetic resonance angiography (3D-TOF MRA), susceptibility-weighted imaging (SWI), fistulous point, cortical venous reflux (CVR), cortical venous ectasia (CVE)

J Southeast Asian Med Res 2024: 8: e0192
https://doi.org/10.55374/jseamed.v8.192

Correspondence to:
Saengruang-Orn S, Department of Radiology, Division of Academic Affairs, Phramongkutklao College of Medicine, Bangkok, Thailand.
E-mail: S_supakajee@yahoo.com

Received: 6 November 2023
Revised: 14 February 2024
Accepted: 17 February 2024

Introduction

Intracranial dural arteriovenous fistulas (DAVFs) are abnormal connections between meningeal arteries and dural venous sinuses or cortical veins. These abnormal connections, or fistulas, allow blood to bypass the capillaries and flow directly into the veins or the dural venous sinus system. This can lead to abnormal flow patterns and decreased blood flow to the brain. DAVFs are rare, occurring in only 10 to 15% of all abnormal blood vessel conditions in the dura mater. They also have a relatively low incidence rate, with an estimated 0.16 cases per 100,000 adult population yearly.[1-3]

DAVF symptoms often depend on the location of the fistula, the type of venous drainage, and the blood flow patterns.[4]The specific treatment plan depends on the fistula's size and location, the symptoms' severity, and the patient's overall health. [5-7]

Cerebral angiogram remains the gold standard for diagnosing and treating DAVFs, including evaluating CVR. In practice, most patients with clinical symptoms typically undergo non-invasive diagnostic imaging, such as computed tomography or magnetic resonance imaging, before DSA. Less than 1% of patients with DAVFs require repeated examinations to assess treatment response and recurrence.[8-9]

The three-dimensional time-of-flight magnetic resonance angiography (3D-TOF MRA) is a non-invasive imaging technique that does not require intravenous contrast administration to diagnose DAVFs. It can evaluate the location of the arterial and venous fistulous areas and the occurrence of CVR, providing high-resolution anatomic and vascular flow information. It can also be used as an alternative to DSA in initially evaluating the characteristics and severity of DAVFs.[10-12]

Susceptibility-weighted imaging (SWI) is another helpful technique to diagnose DAVFs and evaluate the location of the shunt. This is because it combines information from phase and magnitude images to highlight the detection of deoxygenated blood with low oxygenation/slow-flowing, creating apparent images of intracranial vessels.[13] Normally, in SWI, venous structures demonstrate hypointense signals due to deoxyhemoglobin, and the arterial system provides a hyperintense signal due to the time-of-flight effect and the absence of the T2* effect.[14] Among patients with DAVFs, the fistulous site may be seen as an area with a hyperintense signal, representing abnormal arterialization of the venous structure. This is based on the principle that veins affected by CVR contain rapidly flowing and nonparamagnetic arterial blood from the arterial fistulous site to the venous structure.[15-17]

Several analytic studies have demonstrated the usefulness of the SWI sequence in detecting intracranial DAVFs but without comparing it with the 3D-TOF MRA. Therefore, this study aimed to evaluate the efficacy of SWI and 3D-TOF MRA in detecting and pretreating intracranial dural arteriovenous fistulas compared with cerebral angiography, the current gold standard for diagnosis and treatment.

Methods

Study design

This retrospective study included patients treated at the Department of Radiology, Phramongkutklao Hospital, between January 2012 and December 2022. The study was approved by the Institutional Review Board, Royal Thai Army Medical Department (IRB number 1269/2022). Due to its retrospective nature, the patient's informed consent was waived.

Subjects and diagnostic procedure

The study included 35 patients with 41 DAVFs undergoing pretreatment MR imaging of the brain and cerebral angiography. All MR imaging scans were obtained using 1.5T scanners (Ingenia; Philips Healthcare) with a standard head coil. The patients were imaged using a routine precontrast brain MR imaging protocol, including axial and sagittal T1WI, axial T2WI, axial SWI, and DWI/ADC sequences, as well as 3D-TOF MRA of the brain and neck. Routine MR imaging protocols using Gd enhancement were obtained in CE MRA, CE-FLAIR and BrainVIEW (Philips AQ: B Healthcare). A standard dose (0.1 mmol/kg) of Gd-DTPA was injected at 1.8 to 2.0 mL/s among all patients using a standard length of IV tubing.

Data collection

The patient's demographic data were obtained from medical records. Data collected comprised sex, age and presenting symptoms. All MR imaging findings were independently reviewed at the PACS workstation by two neuroradiologists with five years of experience in brain MR imaging. The neuroradiologists were blinded to patient data and angiographic diagnoses.

First, we evaluated the SWI, where the fistulous point was identified using an abnormal hyperintense signal within the dural venous sinus or cortical veins. An abnormal hyperintense signal in the venous structures adjacent to the fistulous point represents CVR. Abnormal increased size and numbers of the perimedullary veins adjacent to the fistulous point identified CVE. Then, on 3D-TOF MRA, the abnormal enlarged/flow-related enhancement in the venous structures (Arterialization) represented a fistulous point. The early filling of the cortical veins and venous sinus adjacent to the fistulous point recognized CVR. The angiographic data were collected from reviewing fistulous site of DAVF, evidence of CVR and CVE by a neurointerventionist with over ten years' experience. Any discrepancies in interpretations of MR imaging were resolved by consensus.

Statistical analysis

All statistical analyses were performed using STATA Version 15.1 Software (StataCorp). The interobserver agreement in evaluating MR imaging characteristics was analyzed using Kappa analysis. A chi-square test was used to ascertain the significance of differences in fistulous point, CVR, and CVE between 3D-TOF MRA, SWI and cerebral angiography. The *p*-value <0.001 was considered a statistically significant difference.

Results

Patient demographics and dural arteriovenous fistula characteristics

Thirty-five patients presented 41 DAVFs from cerebral angiography. In total, 15 (36.6%) of DAVFs revealed cavernous sinus location, and 26 (63.4%) indicated convexity location. Two DAVFs in each person were found among four patients (4; 11.4%) and three DAVFs in each were identified in one patient (1, 2.9%). According to the Cognard classification system, DAVFs were categorized as type I (n = 7; 17.1%), type IIa (n = 6; 14.6%), type IIa+b (n = 15; 36.6%), type IIb (n = 3; 7.3%), type IV (n = 8; 19.5%), and type V (n = 2; 4.9%). Slow flow or low-grade fistulas in cavernous sinus locations (n = 2, 4.8%, Cognard I) were not identified on MR imaging. All demographics and DAVF characteristics are shown in **Table 1.**

Accuracy of SWI and 3D-TOF MRA for detecting fistulous points in convexity and cavernous sinus location

Concerning convexity location **(Figures 1 and 2)**, both SWI and 3D-TOF MRA demonstrated high sensitivity (81.8 and 86.4%, respectively) with excellent specificity (100 and 100%, respectively), positive predictive value (PPV) (100 and 100%, respectively), high negative predictive value (NPV) (76.5 and 81.3%, respectively), and high accuracy (91.4% and 94.3%, respectively) in detecting fistulous point without statistically significant differences.

Regarding cavernous sinus location **(Figure 3)**, 3D-TOF MRA exhibited high sensitivity in detecting fistulous points (92.9%), which was significantly higher than that in SWI (35.7%) ($p < 0.001$). 3D-TOF MRA also showed high specificity (95.2), PPV=92.9, NPV=95.2, and accuracy (94.3) in detecting fistulous points **(Table 2).** The interobserver agreement was perfect for interpreting fistulous points on SWI and 3D-TOF MRA, with k value=1.0.

Accuracy of SWI and 3D-TOF MRA for Detecting CVR, CVE, arterial feeder and venous drainers

Both SWI and 3D TOF-MRA demonstrated high sensitivity (83.3 and 87.5%, respectively) and low specificity (54.5 and 36.4%, respectively), fair PPV (80 and 75%, respectively), moderate NPV (60 and 57.1%, respectively) and fair accuracy (74.3 and 71.4%, respectively) in detecting CVR without statistically significant differences. The interobserver agreement was excellent for interpreting CVR on both SWI and 3D-TOF MRA, with k value = 0.93.

Table 1. Demographic data of enrolled patients

Characteristic	No. of subjects (n = 35)
Age, median = 55 (min=2, max=84)	
≤ 45	9 (25.7%)
> 45	26 (74.3%)
Sex	
Male	17 (48.6%)
Female	18 (51.4%)
Clinical presentation	
Altered consciousness	3 (8.6%)
Clonic muscle contraction	1 (2.9%)
Headache	3 (8.6%)
Orbital symptoms	13 (37.1%)
Seizure	4 (11.4%)
Syncope	1 (2.9%)
Pulsatile tinnitus	9 (25.7%)
Vertigo	1 (2.9%)
Cognard Classification	**No. of DAVFs (n = 41)**
I	7 (17.1%)
IIa	6 (14.6%)
IIa+b	15 (36.6%)
IIb	3 (7.3%)
IV	8 (19.5%)
V	2 (4.9%)
Multiplicity	**No. of Cases (n = 35)**
1 DAVFs	30 (85.7%)
2 DAVFs	4 (11.4%)
3 DAVFs	1 (2.9%)
Location	**No. of DAVFs (n = 41)**
Cavernous sinus	15 (36.6%)
Convexity	
Transverse-sigmoid sinus	13 (31.7%)
Superior sagittal sinus	3 (7.3%)
Torcular herophili	2 (4.9%)
Others	8 (19.5%)

SWI exhibited high sensitivity in detecting CVE (87.5%), which was significantly higher than that in 3D-TOF MRA (12.5%) ($p < 0.001$). SWI demonstrated fair specificity (70.4%), low specificity (46.7%), high NPV (95%), and fair accuracy (74.3%) in the detection of CVE. 3D-TOF MRA also showed high specificity (96.3%), low PPV (50%), fair NPV (78.8%), and fair accuracy (77.1%) in detecting CVE. The interobserver agreement was excellent for interpreting CVE on both SWI and 3D-TOF MRA, with k value = 0.88.

The 3D TOF-MRA demonstrated moderate detection of arterial feeders (20/35, 57%) and

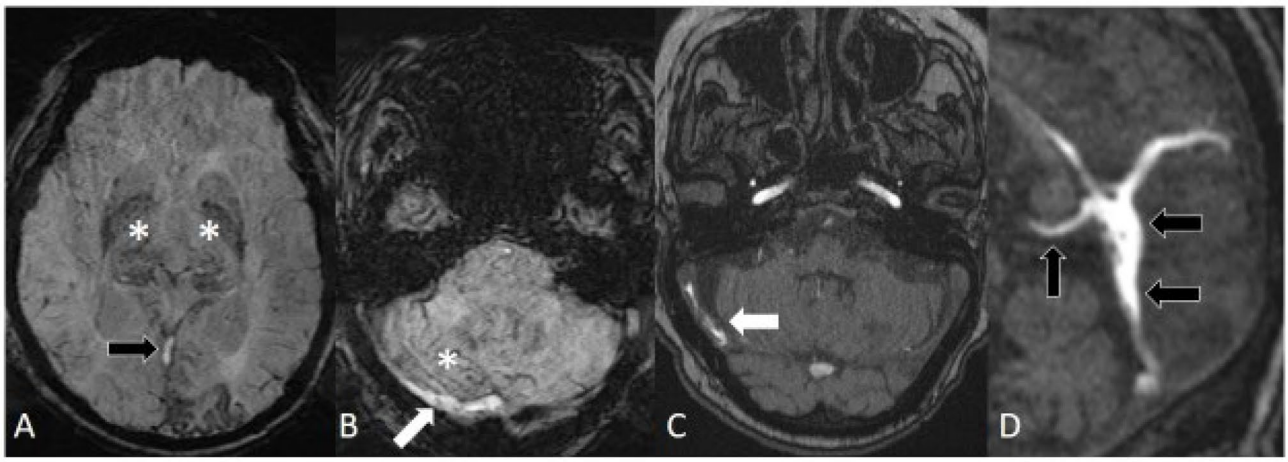

Figure 1. DAVFs at convexity location (Cognard IV). SWI (A and B) and 3D-TOF MRA (C and D) demonstrate a fistulous point (white arrows) at the right transverse sinus, seen as abnormal arterialization. CVR (Black arrows) in the straight sinus, cortical veins, internal cerebral veins, and CVE (asterisks) in SWI at the right cerebellum and bilateral thalami are also seen**.**

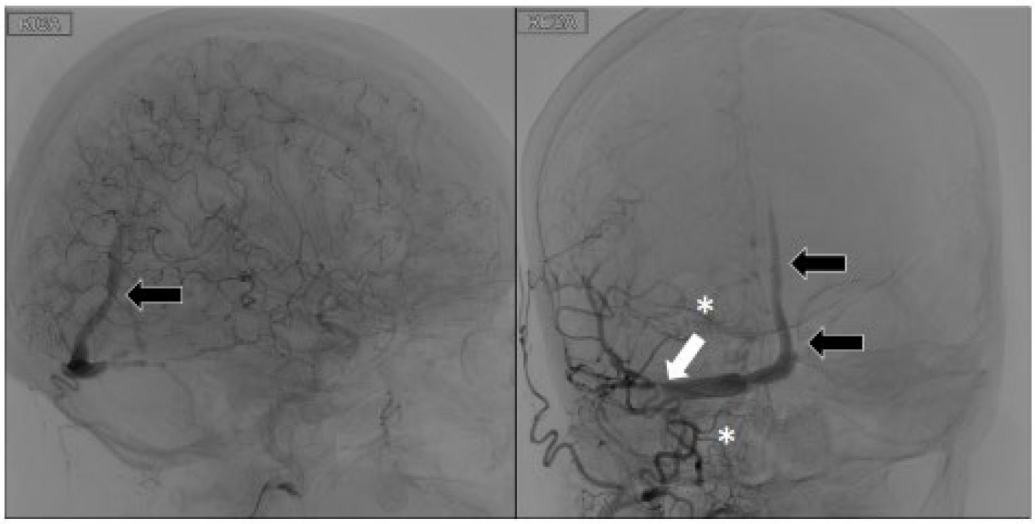

Figure 2. DAVF at convexity location (Cognard IV) (cont.). A cerebral angiogram demonstrates a fistulous point at the right transverse sinus (white arrow), which arterial feeders from a right occipital artery, branched at the right middle meningeal artery and drain into the right transverse sinus as well as CVR in the straight sinus (Black arrows). CVE is also identified (asterisks).

high detection of the venous drainers (33/35, 94.3%), which was significantly higher than SWI (2/35, 5.7%, 22/35, 62.9%) with $p < .001$ **(Table 3)** as well as perfect agreement of interpretation with k value = 1.

Discussion

Early detection of DAVFs associated with CVR is crucial due to the high risk of both hemorrhagic and non-hemorrhagic events and the possibility of treatment to improve outcomes. The initial radiological evaluation should provide comprehensive information to evaluate disease severity and develop a treatment plan effectively. The value of using the SWI sequence in detecting DAVFs has been established in related studies.[15-16] However, our study showed limited evaluation of the slow flow or low-grade DAVFs in both SWI and 3D-TOF MRA.

For high-grade DAVFs (Cognard II-IV), both SWI and 3D-TOF MRA demonstrated high accuracy in detecting the fistulous point at convexity locations. However, the 3D-TOF MRA exhibited better accuracy and sensitivity in detecting

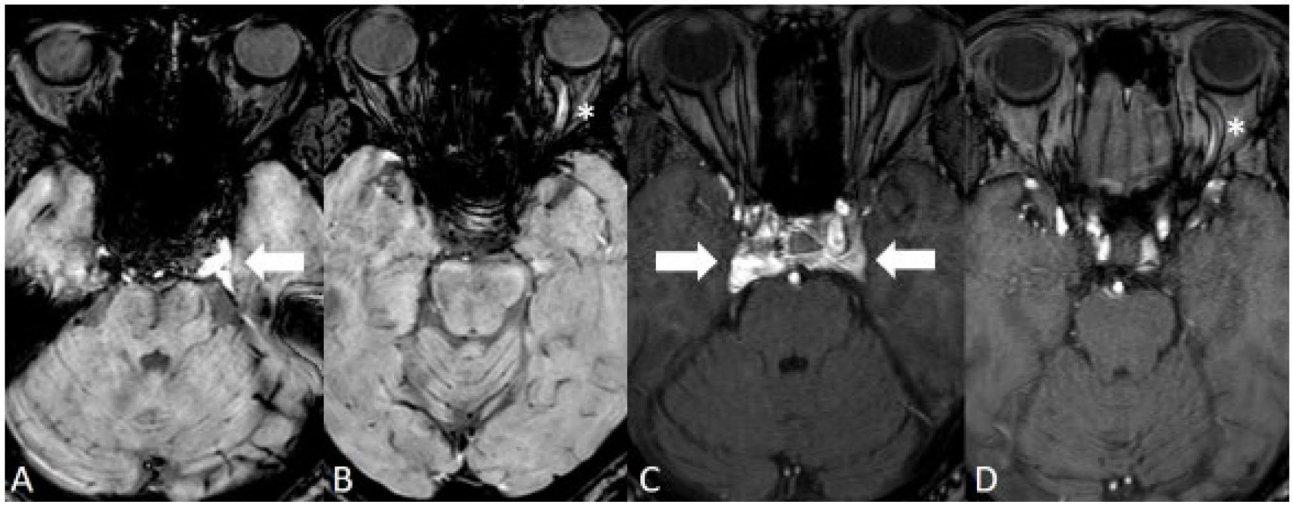

Figure 3. DAVFs at cavernous sinus location (Cognard IIa+b). SWI (A) exhibits a fistulous point at the left cavernous sinus (white arrow). The 3D-TOF MRA (C) also shows fistulous points in both cavernous sinuses (white arrows), superior to SWI. SWI and 3D-TOF MRA (B and D) demonstrate CVR in the left superior ophthalmic vein (asterisk). No CVE is observed.

Table 2. The accuracy of SWI and 3D-TOF MRA in detecting the fistulous points in the cavernous sinus and convexity locations.

Convexity location	**SWI (95% CI)**	**MR (95% CI)**	***p*-value**
Sensitivity	81.8% (59.7, 94.8)	86.4% (65.1, 97.1)	0.677
Specificity	100.0% (75.3, 100)	100.0% (75.3, 100)	-
PPV	100.0% (81.5, 100)	100.0% (82.4, 100)	-
NPV	76.5% (50.1, 93.2)	81.3% (54.4, 96)	0.736
Accuracy	91.4% (81.7, 100)	94.3% (86.2, 100)	0.638
Cavernous sinus location	**SWI (95% CI)**	**MRA (95% CI)**	***p*-value**
Sensitivity	35.7% (12.8, 64.9)	92.9% (66.1, 99.8)	<0.001*
Specificity	100.0% (83.9, 100)	95.2% (76.2, 99.9)	0.310
PPV	100.0% (47.8, 100)	92.9% (66.1, 99.8)	0.541
NPV	70.0% (50.6, 85.3)	95.2% (76.2, 99.9)	0.026
Accuracy	74.3% (59.1, 89.5)	94.3% (86.2, 100)	0.022

PPV= Positive predictive value, NPV= Negative predictive value

the fistulous point at cavernous sinus locations than SWI. 3D-TOF MRA also exhibited superior detection than SWI of arterial feeders and venous drainers.

In this study, SWI demonstrated higher sensitivity in detecting CVE than 3D-TOF MRA. The CVE reflected chronic venous congestion, dilated and tortuous leptomeningeal and/or involved perimedullary vessels (pseudophlebitic pattern). It also increases the risk of rupture, which may result in local mass effects or brain edema[19-20]. SWI plays a critical role in evaluating DAVFs, specifically in convexity locations.

We found that SWI exhibited fair sensitivity in detecting CVR at convexity and cavernous sinus locations, probably due to its limitations in detecting slow-flow DAVFs and the rapid dilution of oxyhemoglobin in congested veins with high deoxyhemoglobin levels. Thus, combining findings from SWI and 3D-TOF MRA exhibited high accuracy in detecting and evaluating high-flow DAVFs in convexity and cavernous sinus locations.

Table 3. The accuracy of SWI and 3D-TOF MRA in Detecting CVR, CVE, arterial feeder, and venous drainers.

CVR (n = 41)	SWI (95% CI)	MRA (95% CI)	*p*-value
Sensitivity	83.3% (62.6, 95.3)	87.5% (67.6, 97.3)	0.680
Specificity	54.5% (23.4, 83.3)	36.4% (10.9, 69.2)	0.394
PPV	80.0% (59.3, 93.2)	75.0% (55.1, 89.3)	0.664
NPV	60.0% (26.2, 87.8)	57.1% (18.4, 90.1)	0.905
Accuracy	74.3% (59.1, 89.5)	71.4% (55.7, 87.2)	0.785
CVE (n = 41)	**SWI (95% CI)**	**MRA (95% CI)**	***p*-value**
Sensitivity	87.5% (47.3, 99.7)	12.5% (0.3, 52.7)	<0.001*
Specificity	70.4% (49.8, 86.2)	96.3% (81, 99.9)	0.011
PPV	46.7% (21.3, 73.4)	50.0% (1.3, 98.7)	0.930
NPV	95.0% (75.1, 99.9)	78.8% (61.1, 91)	0.110
Accuracy	74.3% (59.1, 89.5)	77.1% (62.5, 91.8)	0.785
n = 35 persons	**SWI**	**MRA**	***p*-value**
Arterial feeders	2 (5.7%)	20 (57.1%)	<0.001*
Venous drainers	22 (62.9%)	33 (94.3%)	<0.001*

PPV= Positive predictive value, NPV= Negative predictive value

Regardless, catheter-based cerebral angiography continues to be the definitive diagnostic and treatment tool for DAVFs due to its ability to accurately depict the DAVF's angioarchitecture, location, and number in all types, the anatomy of ECAs and their dural branches, the presence or absence of CVR/CVE and the degree of dural sinus stenosis/occlusion.

Our study encountered several limitations, including its single-institution nature and 1.5T scanners, which probably limited the evaluation of low-grade DAVFs and a small number of cases. However, this study provided essential roles for SWI in evaluating DAVFs, specifically detecting the CVE in convexity locations.

Conclusion

SWI and 3D-TOF MRA help evaluate high-flow DAVFs (Cognard II-IV). SWI is superior in detecting CVE (pseudophlebitic pattern) in convexity locations but needs to be improved in evaluating the fistulous point in cavernous sinus locations. Thus, combining findings from SWI and 3D-TOF MRA exhibit high accuracy in detecting and pretreating the high-flow DAVFs.

Conflict of interest

The authors declare they have no conflicts of interest.

References

1. Kim MS, Han DH, Kwon OK, Oh CW, Han MH. Clinical characteristics of dural arteriovenous fistula. J Clin Neurosci 2002; 9: 147-55. doi: 10.1054/jocn.2001.1029.
2. Lasjaunias P, Chiu M, ter Brugge K, Tolia A, Hurth M, Bernstein M. Neurological manifestations of intracranial dural arteriovenous malformations. J Neurosurg 1986; 64: 724-30. doi: 10.3171/jns.1986.64.5.0724.
3. Lin YH, Lin HH, Liu HM, Lee CW, Chen YF. Diagnostic performance of CT and MRI on the detection of symptomatic intracranial dural arteriovenous fistula: a meta-analysis with indirect comparison. Neuroradiology 2016; 58: 753-63. doi: 10.1007/s00234-016-1696-8.
4. Newton TH, Cronqvist S. Involvement of dural arteries in intracranial arteriovenous malformations. Radiology 1969; 93: 1071-8. doi: 10.1148/93.5.1071.
5. Söderman M, Pavic L, Edner G, Holmin S, Andersson T. Natural history of dural arteriovenous shunts. Stroke 2008; 39: 1735-9. doi: 10.1161/STROKEAHA.107.506485.
6. Gross BA, Du R. The natural history of cerebral dural arteriovenous fistulae. Neurosurgery 2012; 71: 594-602. discussion -3. doi: 10.1227/NEU.0b013e31825eabdb.

7. van Dijk JM, terBrugge KG, Willinsky RA, Wallace MC. Clinical course of cranial dural arteriovenous fistulas with long-term persistent cortical venous reflux. Stroke 2002; 33: 1233-6. doi: 10.1161/01.str.0000014772.02908.44.
8. Kaufmann TJ, Huston J, 3rd, Mandrekar JN, Schleck CD, Thielen KR, Kallmes DF. Complications of diagnostic cerebral angiography: evaluation of 19,826 consecutive patients. Radiology 2007; 243: 812-9. doi: 10.1148/radiol.2433060536.
9. Cloft HJ, Joseph GJ, Dion JE. Risk of cerebral angiography in patients with subarachnoid hemorrhage, cerebral aneurysm, and arteriovenous malformation: a meta-analysis. Stroke 1999; 30: 317-20. doi: 10.1161/01.str.30.2.317.
10. Meckel S, Maier M, Ruiz DS, Yilmaz H, Scheffler K, Radue EW, et al. MR angiography of dural arteriovenous fistulas: diagnosis and follow-up after treatment using a time-resolved 3D contrast-enhanced technique. AJNR Am J Neuroradiol 2007; 28: 877-84.
11. Azuma M, Hirai T, Shigematsu Y, Kitajima M, Kai Y, Yano S, et al. Evaluation of intracranial dural arteriovenous fistulas: comparison of unenhanced 3T 3D time-of-flight MR angiography with digital subtraction angiography. Magn Reson Med Sci 2015; 14: 285-93. doi: 10.2463/mrms.2014-0120.
12. Churojana A, Lakkhanawat S, Chailerd O, Boonchai T, Cognard CC. Cranial dural arteriovenous fistulas: can noninvasive imaging predict angiographic findings? Siriraj Medical J 2018; 70: 289–97.
13. Haacke EM, Xu Y, Cheng YC, Reichenbach JR. Susceptibility weighted imaging (SWI). Magn Reson Med 2004; 52: 612-8. doi: 10.1002/mrm.20198.
14. Haacke EM, Mittal S, Wu Z, Neelavalli J, Cheng YC. Susceptibility-weighted imaging: technical aspects and clinical applications, part 1. AJNR Am J Neuroradiol 2009; 30: 19-30. doi: 10.3174/ajnr.A1400.
15. Hodel J, Gerber S, Zins M, Rodallec M, Leclerc X, Blanc R, et al. MR imaging findings in intracranial dural arteriovenous fistula shunt with retrograde cortical venous drainage using susceptibility-weighted angiography. AJNR Am J Neuroradiol 2011; 32: E196-7. doi: 10.3174/ajnr.A2875.
16. Letourneau-Guillon L, Krings T. Simultaneous arteriovenous shunting and venous congestion identification in dural arteriovenous fistulas using susceptibility-weighted imaging: initial experience. AJNR Am J Neuroradiol 2012; 33: 301-7. doi: 10.3174/ajnr.A2777.
17. Jagadeesan BD, Delgado Almandoz JE, Moran CJ, Benzinger TL. Accuracy of susceptibility-weighted imaging for the detection of arteriovenous shunting in vascular malformations of the brain. Stroke 2011; 42: 87-92. doi: 10.1161/STROKEAHA.110.584862.
18. Saini J, Thomas B, Bodhey NK, Periakaruppan A, Babulal JM. Susceptibility-weighted imaging in cranial dural arteriovenous fistulas. Am J Neuroradiol 2009; 30: e6-e. doi: 10.3174/ajnr.A1265.
19. Nakagawa I, Taoka T, Wada T, Nakagawa H, Sakamoto M, Kichikawa K, et al. The use of susceptibility-weighted imaging as an indicator of retrograde leptomeningeal venous drainage and venous congestion with dural arteriovenous fistula: diagnosis and follow-up after treatment. Neurosurg 2013; 72: 47-54; discussion 5. doi: 10.1227/NEU.0b013e318276f7cc.
20. Jain NK, Kannath SK, Kapilamoorthy TR, Thomas B. The application of susceptibility -weighted MRI in pre-interventional evaluation of intracranial dural arteriovenous fistulas. J Neurointerv Surg 2017; 9: 502-7. doi: 10.1136/neurintsurg-2016-012314.
21. Chen JC, Tsuruda JS, Halbach VV. Suspected dural arteriovenous fistula: results with screening MR angiography in seven patients. Radiology 1992; 183: 265-71. doi: 10.1148/radiology.183.1.1549684.
22. Farb RI, Agid R, Willinsky RA, Johnstone DM, Terbrugge KG. Cranial dural arteriovenous fistula: diagnosis and classification with time-resolved MR angiography at 3T. Am J Neuroradiol 2009; 30: 1546-51 doi: 10.3174/ajnr.A1646.